ISSN 1021-4437, Russian Journal of Plant Physiology, 2010, Vol. 57, No. 5, pp. 599–608. © Pleiades Publishing, Ltd., 2010.
Original Russian Text © A.A. Bulychev, W.J. Vredenberg, 2010, published in Fiziologiya Rastenii, 2010, Vol. 57, No.5, pp. 643–653.

RESEARCH PAPERS

Induction Kinetics of Photosystem I-Activated P700 Oxidation in Plant Leaves and Their Dependence on Pre-Energization

A. A. Bulychev[a] and W. J. Vredenberg[b]

[a] *Department of Biophysics, Faculty of Biology, Moscow State University, Moscow, 119991 Russia; fax: 7 (495) 939-1115; e-mail: bulychev@biophys.msu.ru*

[b] *Laboratory of Plant Physiology, Wageningen University and Research, Droevendaalsesteeg 1, 6708 PB Wageningen, The Netherlands*

Received October 27, 2009

Abstract—Absorbance changes ΔA_{810} were measured in pea (*Pisum sativum* L., cv. Premium) leaves to track redox transients of chlorophyll P700 during and after irradiation with far red (FR) light under various preillumination conditions in the absence and presence of inhibitors and protonophorous uncoupler of photosynthetic electron transport. It was shown that cyclic electron transport (CET) in chloroplasts of pea leaves operates at its highest rate after preillumination of leaves with white light and is strongly suppressed after preillumination with FR light. The FR light-induced suppression was partly released during prolonged dark adaptation. Upon FR illumination of dark-adapted leaves, the induction of CET was observed, during which CET activity increased to the peak from the low level and then decreased gradually. The kinetics of P700 oxidation induced by FR light of various intensities in leaves preilluminated with white light were fit to empirical sigmoid curves containing two variables. In leaves treated with a protonophore FCCP, the amplitude of FR light-induced changes ΔA_{810} was strongly suppressed, indicating that the rate of CET is controlled by the pH gradient across the thylakoid membrane.

Key words: Pisum sativum, cyclic electron flow, redox state of P700, thylakoid ΔpH, methyl viologen, protonophore.

DOI: 10.1134/S1021443710050018

INTRODUCTION

Photosystem I (PSI) of plant chloroplasts is known to support cyclic electron transport (CET) in addition to main electron flow from water to $NADP^+$ and other alternative acceptors [1–3]. In the presence of some redox mediators, CET in isolated chloroplasts is coupled with reversible uptake of a charged cofactor from the medium, which simplifies the observation and characterization of artificial CET [4]. The identification of CET in intact leaves is more difficult, because each component in the electron transport chain (ETC) both accepts and donates electrons, so that the redox state of electron carriers, depending on the excitation rate of the chain, may persist unaltered for a long time. Despite methodological complications, it is becoming increasingly evident that CET plays an important role in bioenergetics and regulation of photosynthesis (see reviews [5, 6]).

According to current notions, CET is capable of generating the electrochemical H^+ gradient in similarity to analogous function of linear electron transport [7]. By this means CET promotes synthesis of extra ATP required for optimal ATP/NADPH ratio [8]. This function can be especially required for starting CO_2 fixation reactions during the induction period of photosynthesis. The creation of proton gradient at the thylakoid membrane during CET may have also a controlling role, because of a supposed suppression of PSII photochemical activity (through nonphotochemical quenching) under excessive irradiance and limited capacities for CO_2 fixation [8, 9]. Furthermore, it is assumed that, upon limited consumption of NADPH in Calvin–Benson cycle, the electron flow at PSI level can be redirected to the cyclic route, thus generating ΔpH and enhancing nonphotochemical quenching in PSII.

One approach to study CET in plant leaves consists in analysis of absorbance changes attributed to redox state of the reaction center chlorophyll of PSI, P700 [3, 10, 11]. The P700 redox state can be monitored from differential absorbance changes at 810 nm with respect to 870 nm (ΔA_{810}) [11]. The approach to CET identification is generally based on the analysis of ΔA_{810} transients induced in the leaf by far red light

Abbreviations: CET—cyclic electron transport; DCMU—3-(3,4-dichlorophenyl)-1,1-dimethylurea; ETC—electron transport chain; LET—linear electron transport; FCCP—carbonyl cyanide *p*-trifluoromethoxyphenylhydrazone; FR—far red; FRL—FR light; FNR—ferredoxin–NADP reductase; MV—methyl viologen; PQ—plastoquinone; PSI and PSII—photosystems I and II; WL—white light.

(FRL) that excites PSI only. Since electron flux from PSII toward PSI is thus prevented, FRL induces almost complete oxidation of P700. In the subsequent dark period, $P700^+$ is slowly reduced owing to the electron flux to P700 through the cyclic pathway and from the stromal donors [12, 13]. The decomposition of the kinetic curve of $P700^+$ dark reduction into several exponential terms provides the means to compare the rates of electron fluxes to $P700^+$ along the cyclic route and from alternative sources [13–15]. Another approach to CET quantification makes use of the leaf exposure to white light (WL) under control conditions and in the presence of methyl viologen (MV), an agent that effectively consumes all electrons available on the acceptor side of PSI, thus excluding CET [15, 16].

Much effort was spent to determine stationary characteristics of CET under various (e.g., stress) conditions and to estimate the contribution of CET to the total electron flux transmitted through PSI [8, 14, 15, 17]. The dynamics of CET changes during the induction period of photosynthesis is a less explored area. By measuring the induction kinetics of ΔA_{810} during and after illumination with FRL, researchers unveiled some important properties of CET and quantified the content of electron donors and acceptors closely associated with PSI [6, 18, 19]. It was observed that the complex kinetics of P700 oxidation in response to FRL is related to temporal variations in proportions between CET and electron flows along alternative pathways from endogenous (stromal) reductants [12, 13]. However, the properties of CET remain insufficiently characterized. Significant influence of ionophores on ΔA_{810} signals observed in some studies suggests that the transmembrane proton gradient in thylakoids might be significant for regulation of CET [20], but this role of ΔpH requires a closer examination. It is not yet clear whether the nonmonotonic kinetics of P700 redox changes during FR irradiation are basically similar to the complex nonmonotonic kinetics of ΔA_{810} observed under the action of WL. Information on the influence of preliminary illumination conditions on CET functioning is far from being complete.

Therefore, the aim of this work was to examine CET properties in leaves of pea plants, based on measurements of FRL-induced ΔA_{810} under variation of some key factors, such as duration of dark adaptation, the length and quality of light during preillumination, and proton conductance of thylakoid membranes. The results provide evidence that, in leaves exposed to FRL after preillumination with WL, CET proceeds at its highest rate in the beginning of FRL exposure and decelerates gradually in prolonged excitation. This deceleration is substantially reduced in the presence of protonophores, i.e., agents that affect the passive proton conductance of and the light-driven proton electrochemical gradient across the thylakoid membrane. By contrast, in dark-adapted leaves, the time dependence of CET during exposure to FRL is bell-shaped with a transient maximum.

MATERIALS AND METHODS

Pea (*Pisum sativum* L., cv. Premium) plants were raised at 25°C under illumination with fluorescent lamps (12-h photoperiod, 1500 lx) on a nutrient medium containing 1 mM $MgSO_4$, 3 mM $Ca(NO_3)_2$, 1.25 mM KNO_3, and 0.9 mM KH_2PO_4. Leaves were sampled from 10- to 14-day-old seedlings. Undetached or excised leaves were adapted to darkness for 15 min at room temperature prior to measurements.

Redox transients of P700 chlorophyll in PSI reaction centers were measured from changes in absorbance difference at 810 and 870 nm (ΔA_{810}) [11] as described in [20] with some modifications. The measuring system consisted of a PAM-101 control unit (100 kHz modulation frequency) and ED-P700DW dual-wavelength emitter–detector unit (Walz, Germany). A branched fiber-optic cable was used to guide modulated measuring beam and actinic light toward the leaf sample and to direct transmitted infrared light to the detector. The leaf was placed between a mirror support and the end of the fiber-optic cable.

The leaf was illuminated with neutral white light (WL) of a Luxeon LXK2-PWN2-S00 light-emitting diode (100 lm, 700 mA, 4100 K; Lumileds, United States). The far-red (FR) light was obtained by insertion of an interference filter (717 nm) in the LED housing or from a 70-W halogen lamp light source fitted with a 717 nm interference filter and an electromagnetic shutter. The photon flux densities provided by the LED source of WL and the source of FR light were 1000 and 100 μmol/(m^2 s), respectively. A Schott KL-1500 illuminator (Germany) was used for preillumination with WL. The length of preillumination was controlled with a PAM-103 unit. The preillumination pulse (1100 μmol/(m^2 s)) was given 10 s before ΔA_{810} measurement. The acquisition of ΔA_{810} signals and the timing control of light pulses from LED source were carried out by means of a PCI-6024E analog–digital convertor (National Instruments, United States) and WinWCP software (Strathclyde Electrophysiology Software).

The kinetic curves of $P700^+$ dark reduction after a FRL pulse were fitted with a sum of three exponentials using analysis options of WinWCP software. Individual components were characterized by their amplitudes (A_1–A_3) and time constants (τ_1–τ_3). The relative amplitude of the fast component, i.e., $A_1/(A_1 + A_2 + A_3)$ was used as a measure of CET activity. The association of the fast component with CET has been revealed [16].

Influence of inhibitors on photoinduced ΔA_{810} signals was examined after infiltration of leaves with artificial pond water (0.1 mM KCl, 1.0 mM NaCl, and 0.1 mM $CaCl_2$) supplemented with chemical agents. To this end, an excised leaf and 20 ml of infiltrating solution were put into a 100-ml glass syringe. The

plunger was drawn repeatedly to create and maintain negative pressure in the syringe. The leaf was infiltrated within about 5–10 min. In test experiments leaves were infiltrated with the solution without reagents. After gentle infiltration all essential features of ΔA_{810} kinetics remained unimpaired, including prompt and delayed oxidoreduction transients induced by intense WL. The amplitude of ΔA_{810} signal in infiltrated leaves was somewhat smaller than in intact leaves because infiltration reduced light-scattering and shortened the optical pathway of measuring light.

Figures represent results of typical experiments performed in at least four replicates. In Fig. 1 each ΔA_{810} signal is an averaged curve obtained from three measurements made under identical conditions. We used 3-(3,4-dichlorophenyl)-1,1-dimethylurea (DCMU) obtained from Serva (Germany) and methyl viologen from Acros Organics (Belgium). Carbonyl cyanide *p*-trifluoromethoxyphenylhydrazone (FCCP) was from Boehringer Mannheim (Germany).

RESULTS

Modulation of P700 Photooxidation by Electron Transport Effectors and Membrane Permeabilizer Reveals Effect on CET

Figure 1 shows the kinetics of ΔA_{810} signals induced by moderate-intensity FRL (40 μmol/(m^2 s)) in leaves adapted to darkness for 10 min (curves *1*) and in leaves preilluminated with either 10-s pulse of FRL plus 30-s darkness (curves *2*) or with 20-s pulse of WL (1100 μmol/(m^2 s)) plus 10-s darkness (curves *3*). Measurements were performed under four sets of experimental conditions: (a) untreated leaf, (b) leaf infiltrated with 200 μM DCMU, (c) infiltration with 250 μM methyl viologen, and (d) infiltration with 5 μM FCCP.

Under control conditions, P700 oxidation induced by a pulse of FRL proceeded slower in a dark-adapted leaf (10 min) (curve *1*) than in a leaf preilluminated for 30 s with FRL (curve *2*). When the leaf was preilluminated for 20 s with WL, the P700 oxidation induced by FRL was strongly delayed and did not reach the stationary level within the observation period (curve *3*). The dark reduction of $P700^+$ was accelerated by this treatment.

In earlier work [6] FRL-induced ΔA_{810} signals similar to curve *2* of Fig. 1a were observed after long (>10 min) preillumination of leaves by light exciting both PSI and PSII. This finding led authors to conclude that the steep photooxidation was observed under conditions with activated ferredoxin–NADP reductase (FNR) and with ETC capable of driving noncyclic electron flow. In our experiments the steep photooxidation of P700 under the action of FRL (curve *2*) was observed under conditions of inactive FNR, because the enzyme-mediated NADP reduction is known to start after 10–20 s of illumination with intense WL. Apparently, the long (>10 min) preconditioning of ETC for linear electron transport is nonessential for P700 oxidation kinetics exemplified in Fig 1a, curve *2*.

It is reasonable to suppose that the delayed S-shaped slow rise of ΔA_{810} in leaves illuminated previously with WL (Fig. 1a, curve *3*) is associated with electron transport that has caused plastoquinone (PQ) reduction during this pretreatment and that the pool of reduced PQ is utilized during FR irradiation as a source of electrons for PSI. In order to check this assumption, we examined P700 photooxidation in leaves infiltrated with DCMU solution. Figure 1b obtained with the DCMU-treated leaf shows that ΔA_{810} kinetic patterns after 10-min darkness and after FR preillumination were quite similar to those in the untreated leaf (curves *1, 2* in Figs. 1a and 1b). On the other hand, DCMU not only inhibited the effect of WL preillumination, observed in untreated leaves, but also acted similarly to FR preillumination (cf. curves *3* in Figs. 1a, 1b). This was apparently due to oxidation of PQ pool during WL exposure. Such influence of DCMU on FRL-induced P700 oxidation indicates that the delayed photooxidation after WL preillumination of untreated leaves is linked to the redox poise of the PQ pool at the start of FRL excitation.

The question arises if a reduced PQ pool is consumed as an electron source for linear electron flow to ferredoxin and available acceptors or whether the reduced PQ promotes the onset and maintenance of CET. To answer this question, we infiltrated leaves with the solution of MV, an extremely effective acceptor that captures electrons from iron–sulfur centers on the acceptor side of PSI thus preventing electron flow to ferredoxin. Figure 1c shows that, in the presence of MV, the kinetics of P700 oxidation induced by FR light in dark-adapted and preilluminated leaves were nearly identical. The lag period observed prior to P700 photooxidation in untreated WL-preilluminated leaves disappeared in the presence of MV, like it did in DCMU-treated leaves (curves *3* in Figs. 1a–1c). The dark reduction of $P700^+$ after the pulse of FR light proceeded notably slower than in untreated leaves and leaves infiltrated with DCMU: the time constant of ΔA_{810} dark relaxation was as long as 7.0–9.5 s. The absence of the lag period after WL preillumination in MV-treated leaves suggests evidence that the lag phase in the kinetics of P700 photooxidation (Fig. 1a, curve *3*) cannot be assigned to linear electron transport (LET) through PSI from the reduced PQ as an electron source. Hence, the initial slow photooxidation of P700 under the action of FRL in control leaves preilluminated with WL is a manifestation of cyclic electron flow driven by PSI. The accelerated dark reduction of $P700^+$ during the light-off response induced at the stage of slow P700 photooxidation supports the conclusion on a higher CET/LET ratio after WL preillumination.

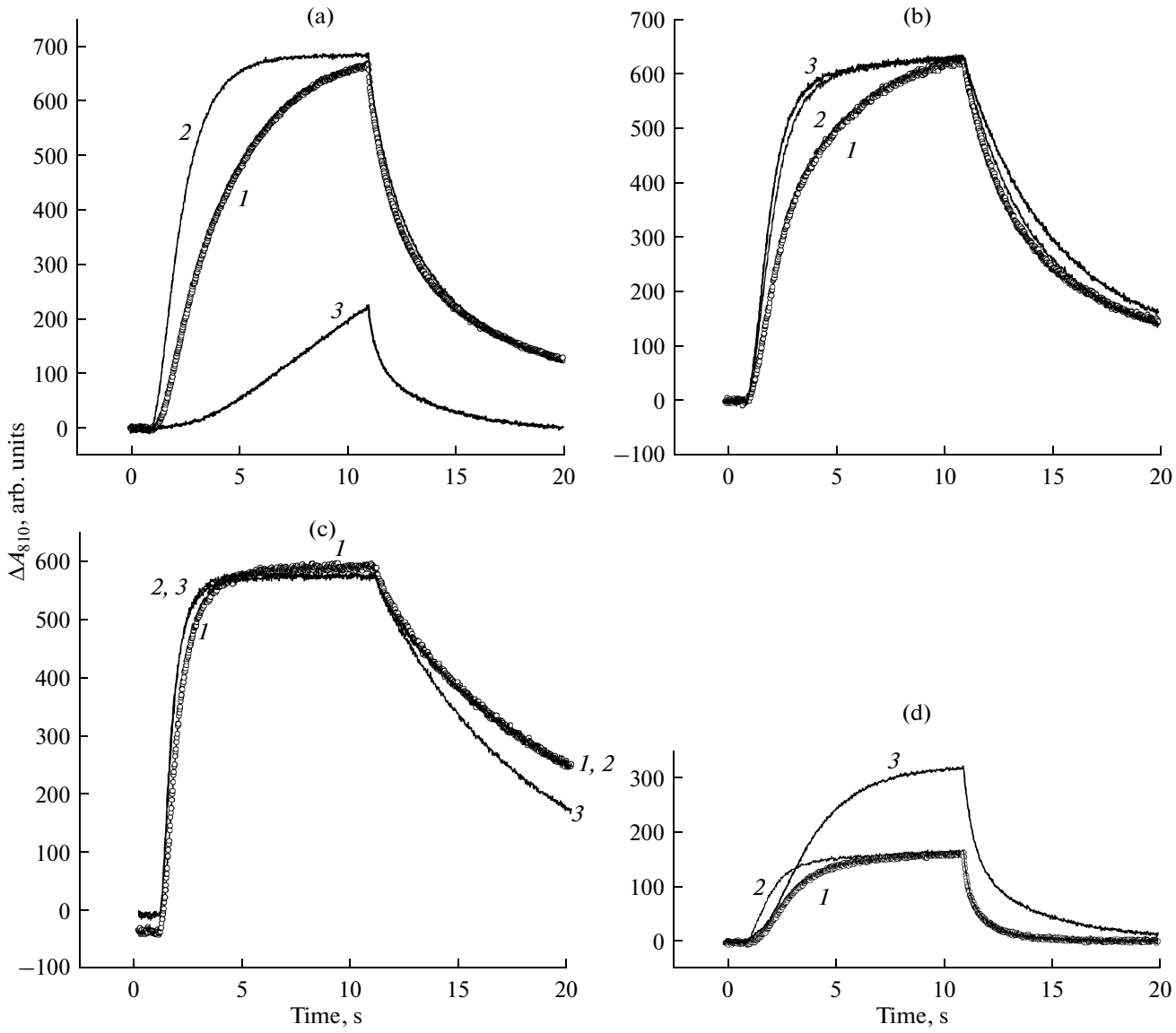

Fig. 1. Kinetics of P700 oxidation induced in pea leaves by far red light (FRL, 40 μmol/(m^2 s)) after 10-min dark adaptation (curves *1*, open circles); 30 s after 10-s preillumination with FRL (curves *2*); and 10 s after 20-s preillumination with white light (WL, 1100 μmol/(m^2 s)) (curves *3*) under different sets of experimental conditions: (a) untreated leaf (control); (b) leaf infiltrated with 0.2 mM 3-(3,4-dichlorophenyl)-1,1-dimethylurea (DCMU); (c) infiltration with 0.25 mM methyl viologen (MV); and (d) infiltration with carbonyl cyanide *p*-trifluoromethoxyphenylhydrazone (FCCP, 5 μM). The FR light was switched on at $t = 1$ s.

Inhibition of CET by MV was manifested not only in a steeper rise of ΔA_{810} but also in a slower dark reduction of P700$^+$ after the FR pulse, as compared to the kinetics of P700$^+$ dark reduction in untreated and DCMU-infiltrated leaves (slow reduction reflects low rate of electron arrivals to P700$^+$ from the stromal reductants). The results presented in Fig. 1a reveal essential features of PSI-driven CET. It can be stated that CET induced by FRL is strongly activated after preillumination of the leaf with WL. The PSI-driven CET gradually decelerates during FR illumination. Consequently, CET is strongly suppressed during the second or repeated exposures of leaf to FRL. The ability of PSI to support CET was notably lower after the dark incubation than in leaves preilluminated with WL (Fig. 1a, curves *1, 3*) The lower CET in a dark-adapted leaf, as compared to CET in a leaf preilluminated with WL, requires further notice. An association with different levels of reduced PQ might be amongst the sources of its regulation.

The functional role ascribed to CET is related to generation in thylakoids of proton-motive force ($\Delta\mu_H$) that contributes to ATP synthesis. Based on this notion, one can expect that ΔpH generation during FR exposure is a principal factor that accounts for CET retardation in parallel with accumulation of pho-

tochemically inactive oxidized form $P700^+$. In order to check this assumption, we infiltrated leaves with the solution of FCCP, a lipophilic H^+ ionophore that elevates membrane conductance for protons and lowers the transmembrane $\Delta\mu_H$ (ΔpH). Figure 1d shows that ΔA_{810} signals induced by FRL in FCCP-treated leaves were considerably smaller for a given time range and light intensity than in control leaves or with other treatments (Figs. 1a–1c). The lack of strong P700 photooxidation in the presence of FCCP suggests that low ΔpH promotes CET operation through balancing the rates of P700 oxidation and P700 reduction (photochemical charge separations and electron fluxes to $P700^+$ from PSI donors, respectively). The light-on rates of ΔA_{810} signals induced by FRL in a dark-adapted and FR-preilluminated leaf differed appreciably, like in untreated leaves (Fig. 1d, curves *1, 2*). The WL preillumination caused a noticeable increase in ΔA_{810} signal induced by a subsequent FR pulse (curve *3*) and a discernibly slower dark relaxation. This is opposite to the effects of WL preillumination in untreated leaves. The suppressed FRL-induced accumulation of $P700^+$ indicates a release of the FRL-driven deceleration (inhibition) of CET in the presence of the protonophore. This in turn would suggest that the FRL-driven deceleration (inhibition) of CET is closely associated with ΔpH formation in the CET pathway.

Dependence of P700 Photooxidation Kinetics on Preillumination Conditions

The kinetic curves of ΔA_{810} signals induced in dark-adapted leaves by FRL of high intensities contain inflection points that are frequently inconspicuous at a lower intensity used in the experiments illustrated in Fig. 1. Under the action of high-intensity FRL, nonmonotonic induction curves of P700 photooxidation are clearly visible [19]. Figure 2a shows the induction curves of P700 photooxidation induced by high-intensity FRL (100 μmol/(m^2 s)) following variable periods of darkness after preceding 10-s FR pulse of the same intensity. The initial changes in P700 redox state, manifested as a transient peak, were followed by a gradual S-shaped accumulation of $P700^+$ to a high steady-state level. These kinetically distinguishable signal components depended in different ways on preillumination conditions. The amplitude of the transient ΔA_{810} peak induced by FRL decreased substantially upon the prolongation of dark period (Fig. 2b). On the other hand, this transient disappeared completely after 20-s preillumination with WL (Fig. 2c). A shorter (200 ms) WL preillumination pulse also caused a strong, though incomplete suppression of this $P700^+$ transient (Fig. 2d).

Unlike the transient peak of P700 photooxidation, the S-shaped slow oxidation phase disappeared after FRL preillumination (Fig. 2, curve *1*), but increased progressively with the length of dark adaptation (Fig. 2a, curves *2–5*), and was manifested in full (without superposition with other components) after WL preillumination (Figs. 2c, 2d). The effects of long dark adaptation and of 20-s WL preillumination on FR-induced ΔA_{810} signals were somewhat similar, since both pretreatments lowered the $P700^+$ level attained by the end of FR pulse and accelerated the dark reduction of $P700^+$ (cf. Fig. 2a, curve *5* and Fig. 2c, curve *2*). When the FR illumination was preceded by a shorter pulse of WL (0.2 s), the rate of $P700^+$ dark reduction was comparable to that in a dark-adapted leaf (Fig. 2d). These observations support the idea that incomplete oxidation of P700 in FRL is due to operation of cyclic electron transport that counteracts photochemical P700 oxidation.

Formal Description of the P700 Oxidation Kinetics in FR Light and Analysis of $P700^+$ Dark Reduction

The sigmoid shape of the kinetic curves of FRL-induced P700 photooxidation in leaves preilluminated with a WL pulse can be fitted with mathematical equations. One of the simplest ones, with only two variables, is the Hodgkin–Huxley equation: $A(t) = A(1 - \exp(-t/\tau))^P$, where A is the amplitude of absorbance change ΔA_{810}, τ is a characteristic time constant related (at constant P) to the delay time and steepness of the response, and P is an empirical fit constant related nearly exclusively to the delay period of $A(t)$ increase at equal τ. Figure 3a is an example of fitting an experimental response with a corresponding simulation curve. The τ value increased strongly at low intensities of FRL. The inverse of τ (rate constant) was roughly proportional to the intensity of FRL (Fig. 3b), indicating that this parameter is related to that of a photochemical process. Such formal description of ΔA_{810} kinetics might be a suitable means to quantify P700 oxidation under the action of FRL after WL preillumination. Validation of a theoretical equation for simulating the experimental curves is required, in which the variables can be given a physiological meaning.

Since $P700^+$ is not expected to accumulate at moderate light excitation rates during CET, it is obvious that CET slows down monotonically as $P700^+$ is observed to accumulate under the action of FRL. This conclusion applies primarily to the case when CET activity is at the highest level just in the beginning of FR pulse (leaves preilluminated with WL, Figs 2c, 2d, and 3a). The initial oxidation transient of nonmonotonic ΔA_{810} signals at high FRL intensities, exemplified in Fig. 2a, seems to represent the oxidation of PSI donor side (electron transfer from the donor to the acceptor side) occurring in excess of CET. In order to clarify the dynamics of CET in dark-adapted leaves, we analyzed the kinetics of ΔA_{810} dark relaxation after FR pulses of various lengths.

In consistency with previous reports [15, 16], the kinetics of dark reduction of $P700^+$, accumulated in

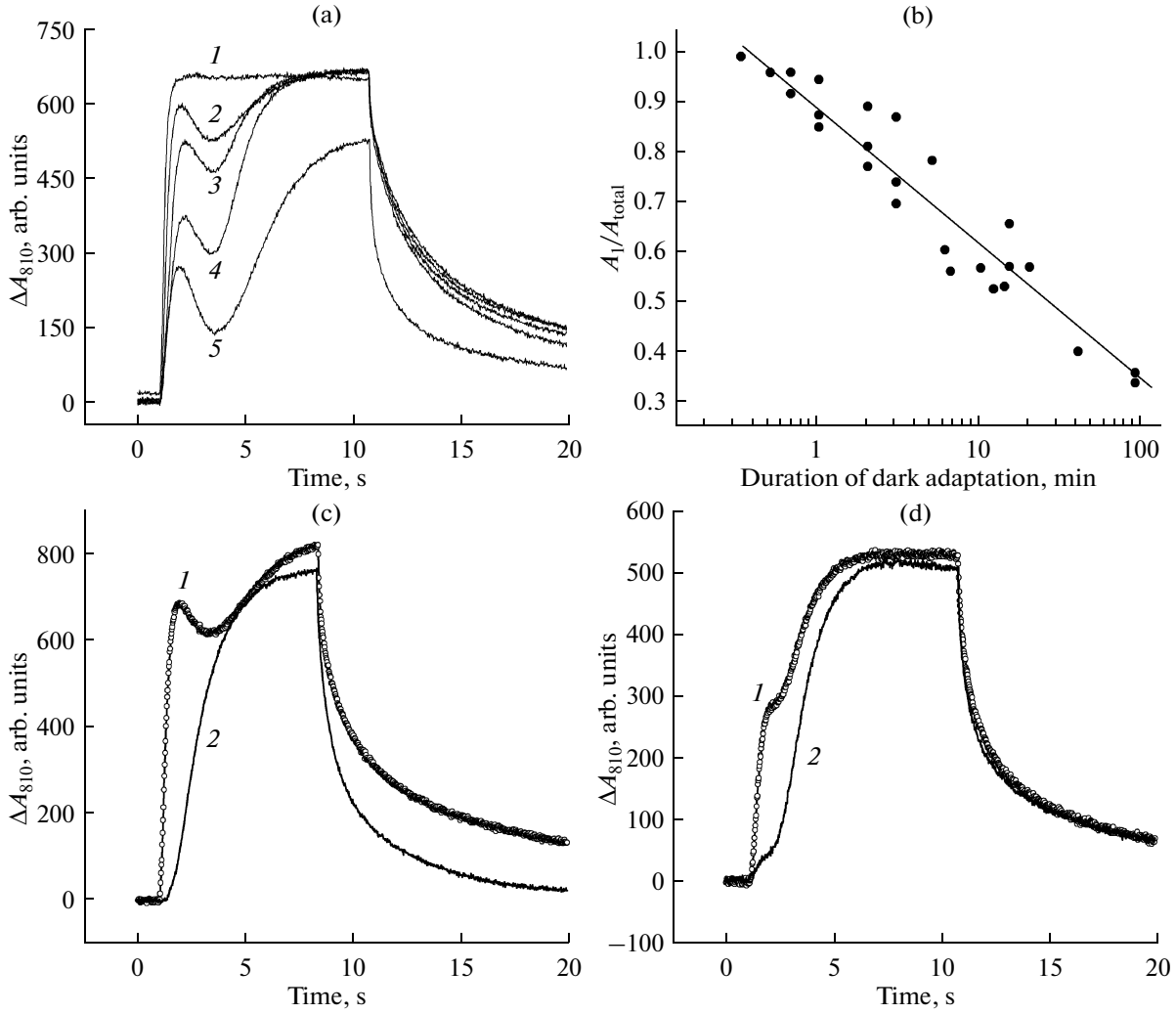

Fig. 2. Effects of preillumination conditions on the kinetics of P700 oxidation during the pulse of FRL (100 μmol/(m^2 s)) and on subsequent dark reduction of P700$^+$ in pea leaves.

(a) Kinetics of FRL-induced P700 oxidation in leaves kept for various dark periods (D) after preliminary 10-s FRL pulse of the same intensity: (1) D = 30 s, (2) D = 2 min, (3) D = 5 min, (4) D = 20 min, (5) D = 40 min.

(b) Relative amplitude of the transient maximum in FRL-induced ΔA_{810} induction curves as a function of length of dark adaptation. A_{total} is the total amplitude of ΔA_{810} transients; A_1 is the amplitude of the initial peak.

(c) Complete suppression of the initial transient in FRL-induced ΔA_{810} signals after preillumination with 20-s pulse of WL (1100 μmol/(m^2 s)). Records *1* and *2* were measured 2 min after FR preillumination and 10 s after 20-s WL preillumination, respectively.

(d) Strong inhibition of the transient "shoulder" in FRL-induced ΔA_{810} signals after preillumination with 0.2-s pulse of WL (1100 μmol/(m^2 s)). Traces *1* and *2* were recorded 6 min after 10-s FR preillumination and 10 s after 0.2-s WL, respectively.

the FR light, fit well to a sum of three exponentials. The fast component with a time constant τ_1 = 150–300 ms is thought to be associated with CET, while slower components (τ_2 ~ 1.5 s and τ_3 ~10 s) correspond to electron flows toward PSI from different stromal sources. We made a componental analysis of the ΔA_{810} dark decay signal as a means to follow CET activity at various stages of the induction curve. Based on this decomposition we determined the amplitude of the fast component in P700$^+$ dark reduction as a function of duration of FR pulse. To this end, the leaf was dark adapted for 7 min prior to each measurement and then a FR pulse of variable length was applied (Fig. 4a). The kinetic curves of ΔA_{810} dark relaxation were then decomposed into individual components and the relative contribution of fast component (CET indicator) to the total signal amplitude was determined. Figure 4b shows the results of this analysis. It can be seen in Figs. 4a and 4b that the relative extent of the fast component, $A_1/(A_1 + A_2 + A_3)$ increased with FRL pulse duration up to approx. 1 s. At this time of the FRL pulse the P700 photooxidation, according to the ΔA_{810} trace,

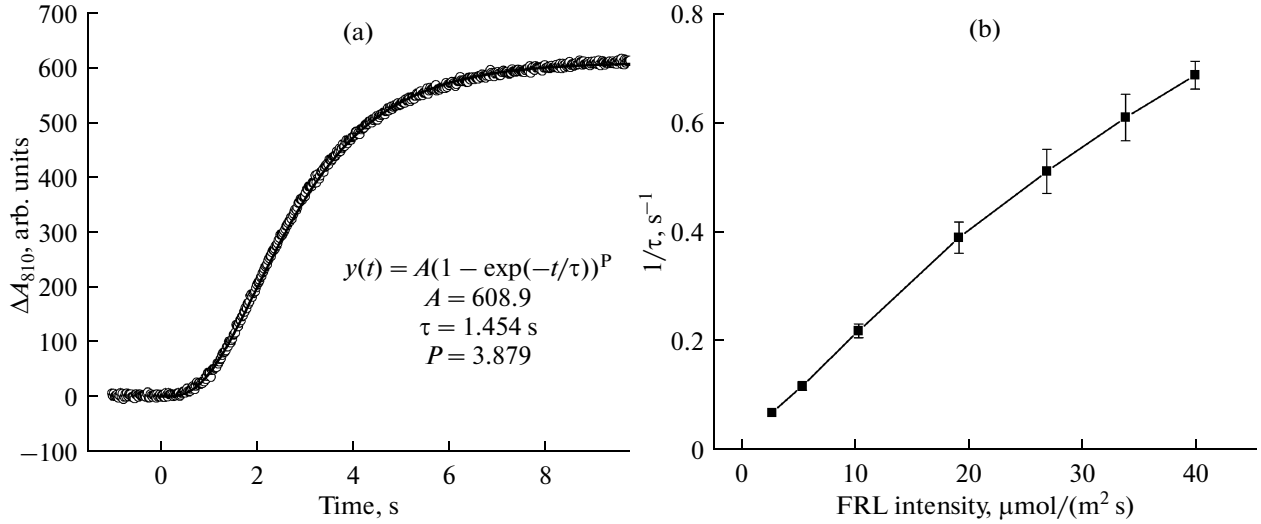

Fig. 3. Kinetics of FRL-induced P700 photooxidation assigned to operation of cyclic electron transport.

(a) Comparison of experimental data and the fitting curve. The pea leaf was dark-adapted for 15 min, preilluminated with 200-ms WL pulse (1100 μmol/(m^2 s)), and exposed after 5 s in darkness to FRL (40 μmol/(m^2 s)). Open circles show experimental data and the solid line is a calculated curve. The inset shows the equation used for data approximation and the values of fitting parameters. The FR light was switched on at $t = 0$.

(b) Inverse of time constant τ for the fitting curves as a function of FRL intensity. The dark-adapted (7 min) pea leaf was preilluminated with WL for 1 s and then irradiated after 10-s dark interval with FRL of various intensities. Data points with bars represent mean values and standard errors of the mean.

shows a transient inflection. As $P700^+$ accumulation after this transient proceeds in a retarded and S-shaped pattern, the relative extent of CET-associated fast component in the kinetics of dark reduction declined gradually. The plot shown in Fig. 4b is consistent with the assumption that CET in dark-adapted chloroplast is rapidly induced under the action of FRL and then decelerates slowly in parallel with accumulation of $P700^+$.

Effect of FCCP on ΔA_{810} Induction Transients under the Action of WL and FRL

Figure 5 shows typical ΔA_{810} transients induced by a pulse of WL in a preilluminated leaf after its infiltration with water in the absence and presence of FCCP. In the absence of the protonophore, ΔA_{810} signal comprised two waves of P700 oxidation. It has been proposed that the second wave of P700 photooxidation in leaves irradiated with WL after WL preillumination is associated with FNR activation [10, 20, 21]. The protonophore FCCP was found to eliminate the second wave of P700 photooxidation.

As illustrated above (see Fig. 1d), FCCP suppressed the amplitude of the S-shaped component of the FR-induced ΔA_{810} signals. According to similarities of FRL- and WL-induced ΔA_{810} reaction kinetics in response to FCCP addition, we presume that the second wave in the WL-induced ΔA_{810} is associated with alterations in CET activity.

DISCUSSION

While analyzing light-induced ΔA_{810} signals in plant leaves, several processes should be considered that occur in association with primary charge separations in PSI: charge recombination in the reaction center, cyclic and linear electron flows, and accumulation of $P700^+$ under deficiency of suitable donors [22]. The delayed and sluggish changes in P700 redox state during FR irradiation after WL preillumination (Figs. 1a, 3a), are not due to low photochemical efficiency of PSI, even though rapid oxidation of P700 induced by intense WL (e.g., Fig. 5) might suggest such an inference. In leaves exposed to FRL after preillumination with WL, high photochemical activity of PSI has been shown to be manifested in effective generation of thylakoid electric potential, while the electrogenic effect was low after preillumination with FRL [23]. From comparison of PSI electrogenic activity as a function of WL or FRL preillumination with the respective patterns of ΔA_{810} (not shown) it is evident that FRL-induced excitation of PSI after preillumination with WL gives rise to effective electrogenesis and insignificant changes in P700 redox state. Conversely, low electrogenic activity of PSI in FRL-preilluminated leaves is paralleled by accumulation of $P700^+$.

The FR-induced ΔA_{810} transients in leaves preilluminated with FRL (Fig. 1a, curve *2*) and in leaves treated with a CET inhibitor methyl viologen (Fig. 1c) were similar, indicating that CET is strongly inhibited after preillumination with FRL. On the other hand,

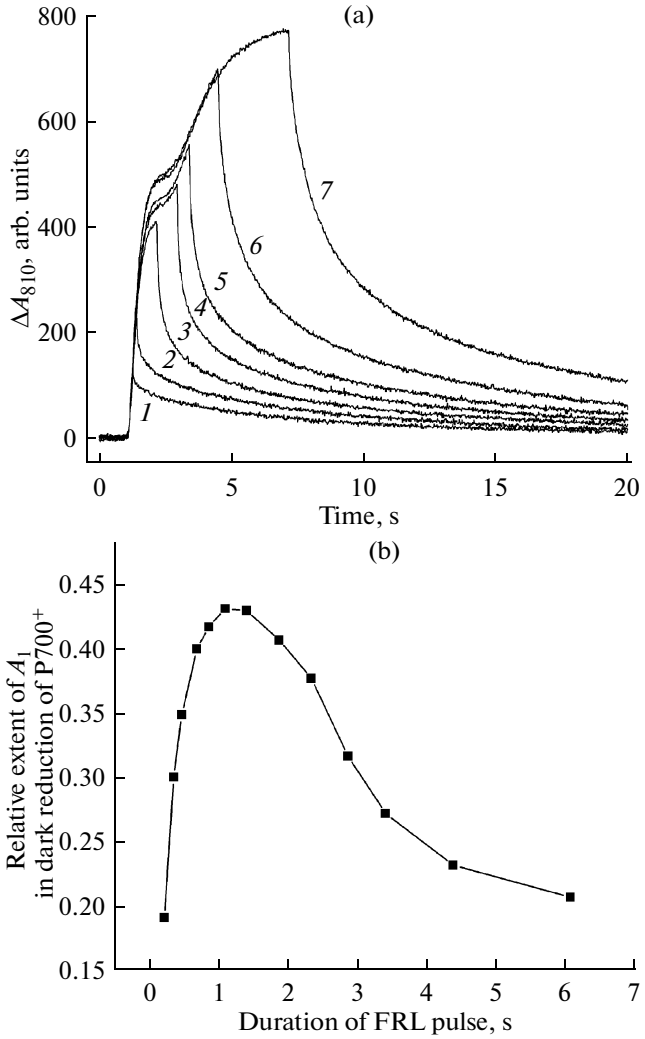

Fig. 4. Dependence of $P700^+$ dark reduction kinetics in pea leaves on the duration of preceding exposure to FRL (100 μmol/(m^2 s)).

(a) Kinetics of ΔA_{810} induced by FRL (100 μmol/(m^2 s)) in leaves adapted for 7 min in darkness and then exposed to a pulse of FRL of variable length; durations of FRL pulses for curves *1*–*7* were 0.22, 0.35, 1.1, 1.9, 2.35, 3.4, and 6.1 s, respectively; (b) relative contribution of the fast component in the signals of $P700^+$ dark reduction ($A_1/(A_1+A_2+A_3)$) dissected at various stages of FR illumination of a dark-adapted (7 min) pea leaf.

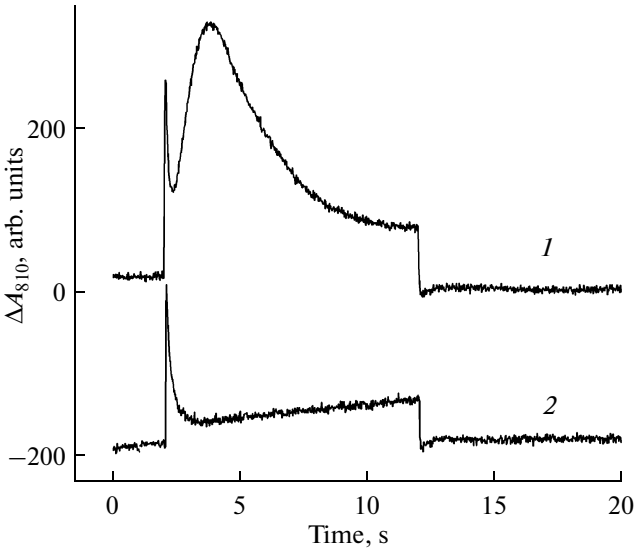

Fig. 5. Effect of the protonophore FCCP on absorbance changes ΔA_{810} induced by white light (WL, 1000 μmol/(m^2 s)) in pea leaves.

(*1*) Multiphase ΔA_{810} transients in water-infiltrated pea leaf exposed to a pulse of WL (1000 μmol/(m^2 s)) given 10 s after 20-s preillumination with WL (1100 μmol/(m^2 s)); (*2*) selective inhibition of the delayed oxidoreduction wave in a similar experiment after leaf infiltration with 10 μM FCCP aqueous solution.

preillumination with WL led to maximal activation of CET, which was manifested in the delayed slow rise of ΔA_{810} (Fig. 1a, curve *3*) susceptible to inhibition by MV (Fig. 1c, *3*). The promotion of CET functioning by preillumination with WL was particularly notable after a long pulse of WL (20 s) but it was also conspicuous after short (0.2 s) periods of WL preillumination (Figs. 2c, 2d). It is thus evident that stimulatory action of WL-preillumination on CET is unrelated to light-dependent activation of electron transport on the acceptor side of PSI (the light period required for activation of FNR is ≥1–10 s) but is mediated and promoted by electron transport-related reactions between PSII and PSI.

The functioning of CET was manifested in the lowered $P700^+$ content at various stages of the induction curve and in the accelerated dark reduction of $P700^+$ (Fig. 1a, curve *3*). Similar changes in the induction curve were introduced by the treatment of leaves with the protonophore FCCP. This provides evidence that CET is coupled with generation of ΔpH and that the backpressure of increasing ΔpH decelerates CET. In dark-adapted leaves, the operation of CET under the action of FRL is largely independent on the presence of DCMU, which is evident from the pairwise comparison of curves *1* and *2* in Figs. 1a and 1b. At the same time, preillumination of DCMU-treated leaf by WL inhibited CET completely, which was apparently caused by oxidation of PQ and other PSI donors during such preillumination (cf. curves *3* in Figs. 1a, 1b).

The nonmonotonic ΔA_{810} transients under the action of high-intensity FRL were previously interpreted as indication of flexibility of electron fluxes that arrive to $P700^+$ during the induction period from several routes and various sources: via CET, from stromal donors, and, possibly, from PSII retaining its residual activity in FRL [19]. While the cause of the transient P700 reduction in leaves illuminated by FRL remains obscure, a shared opinion exists on the origin of fast oxidation of P700 in dark-adapted leaves exposed to FRL. This stage is interpreted to reflect the uncom-

pensated displacement of electrons from PSI donors to the acceptor side of PSI (ferredoxin + FNR) [19]. The total electron capacity of the acceptor side is estimated as 6–8 electrons per P700, whereas the PSI donor side (P700 + plastocyanin) accommodates 4 electrons per P700 [19].

The S-shaped curve of P700 oxidation shown in Fig. 3a reflects the dynamics of CET in the "pure form," without contamination with other components. After a WL prepulse, the rate of electron flow is at its highest in the initial part of the induction curve and slows down along with ΔpH formation, depletion of photochemically active form P700, and inevitable leakage of electrons from cyclic pathway to alternative acceptors (O_2, nitrite, etc.). The S-shaped kinetics (Fig. 3a) fit to an equation comprising a time constant τ and a parameter *P*, related presumably to the rate of ΔpH generation. The meaning of these parameters still awaits interpretation and warrants further study.

In leaves preilluminated with WL, CET operates at its maximal rate immediately after the onset of FRL. By contrast, CET induced by FRL in dark-adapted leaves was characterized by low initial rate. Indeed, the fast component in the dark reduction of $P700^+$, attributed to CET [16], increased within 1–1.5 s of FR illumination, prior to the subsequent gradual decline (Fig. 4b).

It has been discussed recently that different components in the complex ΔA_{810} transients induced by FRL, like those shown in Fig. 2, are possibly attributed to different pools of PSI reaction centers performing cyclic or linear electron transport [8]. However, in later studies this view has been revised [19, 24]. Indeed, if the contributions from different reaction center pools were additive, the inhibition of one or another component of ΔA_{810} signal after preillumination with WL or FRL (see Figs. 2a and 2c) should have resulted in a marked drop of the total ΔA_{810} amplitude. In fact, these pretreatments had almost no effect on the total amplitude of the ΔA_{810} signals. This gives room for the following hypothesis. Energy conversion capabilities and function of PSI are based upon a dynamic heterogeneity of its reaction centers performing cyclic or linear electron transport [24]. The dynamic properties of this complementary heterogeneity are illustrated by and can be understood from the kinetic profiles of the FRL-induced ΔA_{810} responses in dependence of (the duration of) light- and dark- pretreatments.

An important task on the way to comprehensive understanding of the processes involved in CET functioning is the development and validation of a mathematical model that would simulate the experimental data accumulated thus far. It should describe the kinetics in terms of rate constants of reactions around PSI and electrochemical effects thereupon. Effects of this kind have been reported to play a crucial role in and around PSII [25].

ACKNOWLEDGMENTS

This work was supported by the Russian Foundation for Basic Research, project no. 07-04-00132.

REFERENCES

1. Schreiber, U., Hormann, H., Asada, K., and Neubauer, C., O_2-Dependent Electron Flow in Spinach Chloroplasts: Properties and Possible Regulation of the Mehler Ascorbate Peroxidase Cycle, *Photosynthesis: From Light to Biosphere*, Mathis, P., Ed., Dordrecht: Kluwer, 1995, pp. 813–818.
2. Joet, T., Cournac, L., Peltier, G., and Havaux, M., Cyclic Electron Flow around Photosystem I in C_3 Plants. *In Vivo* Control by the Redox State of Chloroplasts and Involvement of the NADH-Dehydrogenase Complex, *Plant Physiol.*, 2002, vol. 128, pp. 760–769.
3. Joliot, P. and Joliot, A., Quantification of Cyclic and Linear Flows in Plants, *Proc. Natl. Acad. Sci. USA*, 2005, vol. 102, pp. 4913–4918.
4. Bulychev, A.A., Voorthuysen, T.V., and Vredenberg, W.J., Transmembrane Movements of Artificial Redox Mediators in Relation to Electron Transport and Ionic Currents in Chloroplasts, *Physiol. Plant.*, 1996, vol. 98, pp. 605–611.
5. Johnson, G.N., Cyclic Electron Transport in C_3 Plants: Fact or Artefact? *J. Exp. Bot.*, 2005, vol. 56, pp. 407–416.
6. Joliot, P. and Joliot, A., Cyclic Electron Flow in C_3 Plants, *Biochim. Biophys. Acta*, 2006, vol. 1757, pp. 362–368.
7. Hald, S., Pribil, M., Leister, D., Gallois, P., and Johnson, G.N., Competition between Linear and Cyclic Electron Flow in Plants Deficient in Photosystem I, *Biochim. Biophys. Acta,* 2008, vol. 1777, pp. 1173–1183.
8. Golding, A.J., Finazzi, G., and Johnson, G.N., Reduction of the Thylakoid Electron Transport Chain by Stromal Reductants – Evidence for Activation of Cyclic Electron Transport upon Dark Adaptation or under Drought, *Planta*, 2004, vol. 220, pp. 356–363.
9. Miyake, C., Miyata, M., Shinzaki, Y., and Tomizawa, K.-I., CO_2 Response of Cyclic Electron Flow around PSI (CEF-PSI) in Tobacco Leaves: Relative Electron Fluxes through PSI and PSII Determine the Magnitude of Non-Photochemical Quenching (NPQ) of Chl Fluorescence, *Plant Cell Physiol.,* 2005, vol. 46, pp. 629–637.
10. Harbinson, J. and Hedley, C.L., Changes in P-700 Oxidation during the Early Stages of the Induction of Photosynthesis, *Plant Physiol.*, 1993, vol. 103, pp. 649–660.
11. Klughammer, C. and Schreiber, U., Measuring P700 Absorbance Changes in the Near Infrared Spectral Region with a Dual Wavelength Pulse Modulation System, *Photosynthesis: Mechanisms and Effects*, Garab, G., Ed., Dordrecht: Kluwer, 1998, pp. 4357–4360.
12. Bukhov, N. and Carpentier, R., Alternative Photosystem I-Driven Electron Transport Routes: Mechanisms and Functions, *Photosynth. Res.*, 2004, vol. 82, pp. 17–33.
13. Egorova, E.A., Drozdova, I.O., and Bukhov, N.G., Modulating Effect of Far-Red Light on Activities of

Alternative Electron Transport Pathways Related to Photosystem I, *Russ. J. Plant Physiol.*, 2005, vol. 52, pp. 709–716.

14. Fan, D.-Y., Hope, A.B., Jia, H., and Chow, W.S., Separation of Light-Induced Linear, Cyclic and Stroma-Sourced Electron Fluxes to $P700^+$ in Cucumber Leaf Discs after Pre-Illumination at a Chilling Temperature, *Plant Cell Physiol.*, 2008, vol. 49, pp. 901–911.
15. Jia, H., Oguchi, R., Hope, A.B., Barber, J., and Chow, W.S., Differential Effects of Severe Water Stress on Linear and Cyclic Electron Fluxes through Photosystem I in Spinach Leaf Discs in CO_2-Enriched Air, *Planta,* 2008, vol. 228, pp. 803–812.
16. Bukhov, N.G. and Egorova, E.A., Identification of Ferredoxin-Dependent Cyclic Electron Transport around Photosystem I Using the Kinetics of Dark $P700^+$ Reduction, *Russ. J. Plant Physiol.*, 2005, vol. 52, pp. 283–287.
17. Clarke, J.E. and Johnson, G.N., *In Vivo* Temperature Dependence of Cyclic and Pseudocyclic Electron Transport in Barley, *Planta*, 2001, vol. 212, pp. 808–816.
18. Oja, V., Eichelmann, H., Peterson, R.B., Rasulov, B., and Laisk, A., Deciphering the 820 nm Signal: Redox State of Donor Side and Quantum Yield of Photosystem I in Leaves, *Photosynth. Res.*, 2003, vol. 78, pp. 1–15.
19. Talts, E., Oja, V., Ramma, H., Rasulov, B., Anijalg, A., and Laisk, A., Dark Inactivation of Ferredoxin-NADP Reductase and Cyclic Electron Flow under Far-Red Light in Sunflower Leaves, *Photosynth. Res.,* 2007, vol. 94, pp. 109–120.
20. Bulychev, A.A., Bezmenov, N.N., and Rubin, A.B., Influence of Electrochemical Proton Gradient on Electron Flow in Photosystem I of Pea Leaves, *Russ. J. Plant Physiol.*, 2008, vol. 55, pp. 433–440.
21. Schansker, G., Srivastava, A., Govindjee, and Strasser, R.J., Characterization of the 820-nm Transmission Signal Paralleling the Chlorophyll *a* Fluorescence Rise (OJIP) in Pea Leaves, *Funct. Plant Biol.*, 2003, vol. 30, pp. 785–796.
22. Ke, B., Photosynthesis, Photobiochemistry, and Photobiophysics, *Advances in Photosynthesis,* vol. 10, Dordrecht: Kluwer, 2001.
23. Bulychev, A.A., Andrianov, V.K., Kurella, G.A., and Litvin, F.F., Photoinduction Kinetics of Electrical Potential in a Single Chloroplast as Studied with Micro-Electrode Technique, *Biochim. Biophys. Acta*, 1976, vol. 430, pp. 336–351.
24. Breyton, C., Nandha, B., Johnson, G.N., Joliot, P., and Finazzi, J., Redox Modulation of Cyclic Electron Flow around Photosystem I in C_3 Plants, *Biochemistry,* 2006, vol. 45, pp. 13 465–13 475.
25. Vredenberg, W., Durchan, M., and Prášil, O., Photochemical and Photoelectrochemical Quenching of Chlorophyll Fluorescence in Photosystem II, *Biochim. Biophys. Acta*, 2009, vol. 1787, pp. 1468–1478.